

## Electronic Structure of a Series of Metals

WALTER A. HARRISON

*General Electric Research Laboratory, Schenectady, New York*

(Received 17 April 1963)

Self-consistent calculations of the electronic structure, including screened exchange, are carried out for Li, Be, Na, Mg, Al, K, and Ca. Results are presented as orthogonalized plane wave (OPW) form factors. They agree well with values of these form factors estimated from splittings at symmetry points in the Brillouin zones obtained from existing band calculations. For calcium, the form factors are used to compute the Fermi surface in detail. The computed form-factor curves may be approximated within a few hundredths of a rydberg by the Fourier transform of a simple one-parameter potential in which the core is replaced by a delta-function repulsive potential. There are no apparent trends in the strength of this repulsion with valence nor with atomic number. The familiar dropping of the even state at the zone face in the alkali metals as the atomic number increases is to be associated with the larger atomic volume rather than with changes in the core potential. An attempt to treat copper in a similar manner indicated that the form-factor approach is quite inadequate for the noble metals.

### I. INTRODUCTION

IN an earlier communication,<sup>1</sup> which we shall call I, it was shown that the Fermi surface of a polyvalent metal and many of its electronic properties are obtainable directly from an "orthogonalized plane wave (OPW) form factor." This single function of wave number (for wave numbers between zero and twice the Fermi wave number) depends only upon the atomic cell volume and the individual ion potential.

If the crystal potential could be written as a sum of simple potentials centered at the ions, the OPW form factor would correspond to the Fourier transform of a single potential. Matrix elements of the Hamiltonian between plane-wave electronic states would then be given by the product of a structure factor, depending only upon the arrangement of the ions and the difference in wave number between initial and final states, and the Fourier transform of a single ionic potential corresponding to that difference in wave number. In the real crystal, the corresponding separation can be made. The same structure factor enters, and a single potential-dependent factor can be defined if we restrict the matrix elements to be between two states at the Fermi surface. We call this factor the OPW form factor.

Because this form factor, which represents a most important aspect of the electronic structure, is independent of the crystal structure it is of interest to compare the curves for a number of metals in the periodic table in order to see any trends in the electronic structure. A series such as sodium, magnesium, aluminum can readily be compared in this way though each has a different crystal structure. It was the hope of seeing trends in electronic structure with atomic number or with valence, as well as the desire to obtain the curves which can be the basis of an understanding of the electronic properties of the metals in question, which motivated the present study. To this end, the OPW form factors were obtained for all nontransition elements through zinc. The curve for copper was

included in the interest of comparison, but was not regarded as useful since approximations in the approach are not appropriate for a noble metal. The curve for zinc was available from previous work,<sup>2</sup> which we will call II.

In Sec. II we define the terms which enter the calculation and indicate the approximations made; a detailed outline of the procedure used is given in Appendix A. In Sec. III we summarize the results for the various metals and compare with existing calculations. In Sec. IV we consider a simple model which describes the results quite well and look for trends with valence and atomic number. A detailed study of the Fermi surface of calcium is given in Appendix B.

### II. CALCULATION OF THE OPW FORM FACTORS

The matrix elements which enter the calculation of many electronic properties are simply the matrix elements of the total Hamiltonian between orthogonalized plane waves. A method was developed in I and II for computing these matrix elements, as well as for computing properties in terms of them. Because orthogonalized waves are not orthogonal to each other, this matrix element will depend upon the zero of energy; in I we selected the zero of energy to optimize the convergence of the perturbation treatment.

We assume that the cores in the metal are the same as in the free ion, and include in the one-particle Hamiltonian, the kinetic energy, a sum of free-ion potentials (one at each ion site), exchange between conduction and core electrons, and the self-consistent field of the conduction electrons. Orthogonality coefficients are obtained using the core wave functions from a Hartree-Fock treatment of the ion.

In I we wrote the matrix elements as matrix elements between plane waves of a pseudopotential  $W(\mathbf{k})$  and separated them into structure-dependent and potential-dependent factors:

$$\langle \mathbf{k} + \mathbf{q} | W(\mathbf{k}) | \mathbf{k} \rangle = S(\mathbf{q}) \langle \mathbf{k} + \mathbf{q} | w(\mathbf{k}) | \mathbf{k} \rangle. \quad (1)$$

<sup>1</sup> W. A. Harrison, Phys. Rev. **129**, 2503 (1963); hereafter referred to as I.

<sup>2</sup> W. A. Harrison, Phys. Rev. **129**, 2512 (1963); hereafter referred to as II.

Here the wave numbers  $\mathbf{k}$  and  $\mathbf{k}+\mathbf{q}$  lie on the Fermi sphere. The structure factor,  $S(\mathbf{q})$ , is given by

$$S(\mathbf{q}) = (1/N) \sum_j e^{-i\mathbf{q}\cdot\mathbf{r}_j}, \quad (2)$$

where the sum is over all  $N$  of the ion positions  $\mathbf{r}_j$ . The OPW form factor,  $\langle \mathbf{k}+\mathbf{q} | w(\mathbf{k}) | \mathbf{k} \rangle$ , is a simple function of  $q$  for  $0 < q < 2k_F$  and is evaluated from the Hartree-Fock field and core wave functions of the ion.

The calculation of these form factors has been described earlier.<sup>1,2</sup> Here we will simply describe the modifications which we have made for the current calculation; these greatly simplify the numerical work. Since the calculations remain rather complex in detail, we give in Appendix A the step-by-step procedure which was used.

In the course of evaluating the form factor, matrix elements of the core potential, including exchange, between plane waves and core wave functions must be evaluated. These can be simplified by noting that the core wave functions,  $\psi_t$ , are solutions of the Schrödinger equation containing this same ionic potential,  $v_{op}'$ ,

$$T\psi_t + v_{op}'\psi_t = \epsilon_t\psi_t,$$

where  $\epsilon_t$  is the customary Hartree-Fock parameter. It is then readily shown that

$$\langle t | v_{op}' | \mathbf{k} \rangle = (\epsilon_t - \hbar^2 k^2 / 2m) \langle t | \mathbf{k} \rangle,$$

so these matrix elements are given directly in terms of the orthogonality coefficients,  $\langle t | \mathbf{k} \rangle$ .

We also require matrix elements of the core potential between plane waves. The core potential includes the self-consistent field of the core which may or may not be tabulated in the literature. If not, the Fourier transform of the charge density is readily calculated, from which the Fourier transform of the potential is directly obtained using Poisson's equation.

$v_{op}'$  also includes exchange between conduction and core electrons. In our earlier treatment of zinc<sup>2,3</sup> this exchange entered as an  $l$ -dependent potential in the Hartree-Fock treatment used by Piper.<sup>4</sup> We would expect to make little error by using instead the approximate treatment of exchange given by Slater<sup>5</sup>; that is, free-electron exchange, and we use that procedure here. In this approximation the exchange potential is given by  $-3e^2(3\rho_0/8\pi)^{1/3}$ , where  $\rho_0$  is the local density of (core) electrons. This, again, may be computed from the tabulated core wave functions, and  $v_{op}'$  becomes a simple potential.

We find the inclusion of exchange in the calculation reasonably important. In Fig. 1 is shown the OPW form factor computed for aluminum with exchange included as described above. In addition, the form factor is shown computed without exchange by using the Hartree parameters, rather than the Hartree-Fock

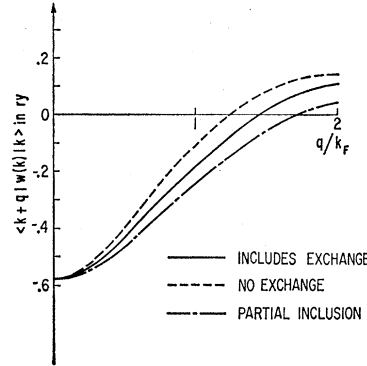


FIG. 1. The OPW form factor for aluminum calculated from the Hartree-Fock field and including exchange; calculated using the Hartree parameters, but including exchange between conduction and core electrons; and calculated from the Hartree parameters omitting exchange between conduction and core electrons.

parameters, and by dropping the exchange in  $v_{op}'$ . The curves are rather close, but differ by as much as  $0.09E_F$  in places. This is considerably larger than the other errors we expect to make and, therefore, the inclusion of exchange is appropriate.

Also shown in Fig. 1 is the form factor obtained including exchange in  $v_{op}'$  but using the Hartree parameters in the computation of  $\langle t | v_{op}' | \mathbf{k} \rangle$ . This is in slightly greater error and suggests that if we treat a metal for which only the Hartree calculation had been done for the ion, it is preferable to omit exchange altogether. This suggestion has been made earlier by Heine.<sup>6</sup>

Finally, we need the self-consistent field arising from the conduction-electron charge distribution. The two interesting contributions to this charge distribution are the deviations from uniform distribution arising from orthogonalizing the plane waves to the core wave functions and those arising from the screening of the core and exchange potentials.

The effect of orthogonalizing all conduction band waves to the core is to localize a charge of

$$(1/N) \sum_{k < k_F} \sum_t \langle \mathbf{k} | t \rangle \langle t | \mathbf{k} \rangle$$

at each core. For the interpolation we used in the treatment of zinc<sup>2</sup> the terms in this sum were independent of  $k$ , and we make that approximation here. We find the number of charges,  $\delta Z$ , localized at each core to be given by  $\delta Z = Z \sum_t \langle \mathbf{k} | t \rangle \langle t | \mathbf{k} \rangle$ , where  $Z$  is the valence (the column number in the periodic table). In our treatment of zinc we concentrated this charge at a point at the nucleus; here we improve on this by distributing it as the core charge is distributed. The fact that this improvement only very slightly modifies our result supports the contention that it is unnecessary to determine the distribution more accurately.

The self-consistent shift of the conduction-band charge density also depends upon the individual behavior of all of the electrons. In II we obtained the shift by integrating over the conduction band. Cohen and Phillips<sup>7</sup> have suggested an approximate treatment

<sup>3</sup> W. A. Harrison, Phys. Rev. **126**, 497 (1962).

<sup>4</sup> W. W. Piper, Phys. Rev. **123**, 1281 (1961).

<sup>5</sup> J. C. Slater, Phys. Rev. **81**, 385 (1951).

<sup>6</sup> V. Heine, Proc. Roy. Soc. (London) **A240**, 340 (1957).

<sup>7</sup> M. H. Cohen and J. C. Phillips, Phys. Rev. **124**, 1818 (1961).

where the appropriate matrix elements are simply divided by the Hartree dielectric function corresponding to the wave number in question. We wish to avoid the determination of matrix elements for states below the Fermi surface, but find the Cohen-Phillips approach inadequate in that it disregards an inherent non-Hermiticity in the matrix elements which arises from

$$v_q^{sc} = \left\{ \frac{4\pi e^2}{q^2 \Omega} \sum_{\mathbf{k} < k_F} \left[ \frac{\langle \mathbf{k} + \mathbf{q} | w(\mathbf{k})^0 | \mathbf{k} \rangle}{T_k - T_{k+q}} + \frac{\langle \mathbf{k} - \mathbf{q} | w(\mathbf{k})^0 | \mathbf{k} \rangle^*}{T_k - T_{k-q}} \right] \right\} / \left\{ 1 - \frac{4\pi e^2}{q^2 \Omega} \sum_{\mathbf{k} < k_F} \left[ \frac{1}{T_k - T_{k+q}} + \frac{1}{T_k - T_{k-q}} \right] \right\}. \quad (3)$$

The sums over the first and second terms in square brackets are identical (a fact which we previously overlooked for the general case), so the square brackets may be contracted to twice the first term. We then replace  $\langle \mathbf{k} + \mathbf{q} | w(\mathbf{k})^0 | \mathbf{k} \rangle$  by  $\langle \mathbf{k} + \mathbf{q} | w(\mathbf{k})^0 | \mathbf{k} \rangle + \frac{1}{2}(T_k - T_{k+q}) \times \sum_t \langle \mathbf{k} + \mathbf{q} | t \rangle \langle t | \mathbf{k} \rangle$ , a form suggested by the form of the non-Hermiticity of the matrix elements. [Note added in proof. Current machine calculations being made of the energy-wave number characteristic for aluminum (to be published) have given incidentally a check on the accuracy of this procedure, and have indicated that it is good to a few thousandths of a rydberg over most of the wave number range.] We then neglect the dependence of the matrix elements upon  $\mathbf{k}$ . Thus, we find the screening field to be given by two terms; the first is  $(1 - \epsilon_q)/\epsilon_q$  times the unscreened matrix element; the second is given by

$$4\pi e^2 Z \sum_t \langle \mathbf{k} + \mathbf{q} | t \rangle \langle t | \mathbf{k} \rangle / [q^2 \Omega_0 \epsilon(q)].$$

This second term, which is absent in the Cohen-Phillips treatment, leads to the correct limiting behavior at long wavelengths.

These modifications were incorporated into the method developed earlier<sup>1-3</sup> to obtain the procedure which is explicitly described in Appendix A.

### III. COMPUTATION AND COMPARISON WITH BAND CALCULATIONS

The computation was carried out in detail for all metals through atomic number 20 (Ca). In all of these metals the core is small, and the approximation that it is the same as in the ion should be quite good. 21 is scandium and begins the first transitions series which

TABLE I. OPW form factors in Ry.

$q/k_F$	0	0.5	1	1.5	2
Li	-0.237	-0.207	-0.137	-0.046	+0.064
Be	-0.703	-0.500	-0.145	+0.124	+0.299
Na	-0.154	-0.145	-0.110	-0.051	-0.001
Mg	-0.353	-0.301	-0.165	-0.009	+0.095
Al	-0.573	-0.427	-0.183	+0.019	+0.113
K	-0.100	-0.104	-0.087	-0.052	-0.014
Ca	-0.231	-0.196	-0.119	-0.036	+0.039
Cu	-0.345	-0.423	-0.336	-0.164	-0.102
Zn	-0.472	-0.329	-0.176	-0.036	+0.074

the nonorthogonality of the orthogonalized plane waves. As a consequence it would lead to a limiting value for small wave numbers of  $-\frac{2}{3}E_F(1 + \sum_t \langle \mathbf{k} | t \rangle \langle t | \mathbf{k} \rangle)$ , whereas we showed in II that the correct value is simply  $-2E_F/3$ ; thus, the Cohen-Phillips approximation leads to errors of the order of 10% in this region. In I we wrote the screening field as

ends in copper. We carried out the analysis for copper, treating the 3d bands as core states though these states actually differ significantly from the corresponding ion states. Finally, we list the results for zinc which were given earlier<sup>2</sup>; in zinc, the core is again rather small.

In each case we computed the form factors for the metal at the observed density. We obtained values for  $q/k_F$  equal to 0, 0.5, 1.0, 1.5, and 2.0. These are given in Table I and plotted in Fig. 2. Before considering trends in the OPW form factors, we shall discuss the calculations for the individual metals and compare the results with existing calculations where possible.

The comparison with existing calculations is not direct. We have obtained matrix elements of the Hamiltonian between two states on the Fermi surface. If the free-electron (or single-OPW) surface intersects a zone face, the OPW form factor for  $q$  equal to the corresponding lattice wave number ( $2\pi$  times the reciprocal lattice vector) equals half the band gap for that zone face, evaluated at this intersection. This neglects modifications of the band gap from interaction with neighboring bands; i.e., it assumes that the wave function can be approximated by the sum of only two plane waves. Errors associated with this

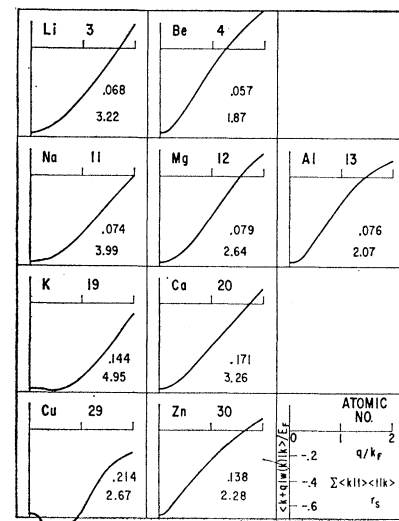


FIG. 2. OPW form factors computed for a series of metals. The key appears to the lower right;  $\sum_t \langle \mathbf{k} | t \rangle \langle t | \mathbf{k} \rangle$  gives a measure of the orthogonality coefficients, or the core size;  $(4\pi r_s^3/3)^{-1}$  is the electron density.

TABLE II. Comparison with band calculations. All energies in Ry.

	$q$	$\langle \mathbf{k} + \mathbf{q}   w(\mathbf{k})   \mathbf{k} \rangle$	Estimate from symmetry-point splitting			Reference
Li	[110]	0.064	0.101 ( <i>N</i> )	0.076 ( <i>P</i> )	0.052 ( <i>H</i> )	10
Be	[100]	0.172	0.093 ( <i>K</i> )	0.155 ( <i>M</i> )		12
	[101]	0.229	0.254 ( <i>H, K</i> )			12
	[002]	0.253	0.247 ( $\Gamma$ )			12
Na	[110]	-0.001	0.008 ( <i>N</i> )	0.018 ( <i>P</i> )	0.026 ( <i>H</i> )	10
Mg	[100]	0.023	0.027 ( <i>K</i> )	0.056 ( <i>H</i> )	0.044 ( <i>M</i> )	15
	[002]	0.046	0.052 ( $\Gamma$ )			15
	[101]	0.069	0.071 ( <i>H</i> )			15
Al	[111]	0.026	0.030, 0.026 ( <i>W</i> )	-, 0.024 ( <i>K</i> )	-, 0.015 ( <i>L</i> )	17, 18
	[200]	0.071	0.055, 0.048 ( <i>W</i> )	-, 0.042 ( <i>K</i> )	0.062, 0.038 ( <i>X</i> )	17, 18
K	[110]	-0.014	-0.016 ( <i>N</i> )	+ 0.020 ( <i>P</i> )	+ 0.039 ( <i>H</i> )	10
Ca	[111]	0.003				
	[200]	0.039				

approximation are expected to be small compared to uncertainties in the potential in most cases.

The band calculations give us energies, or band gaps, at symmetry points. Again neglecting the interaction with neighboring bands, we may deduce splittings associated with the zone faces which intersect this point, but now evaluated at the symmetry point rather than at the Fermi surface. We have shown in II (Fig. 1) that these matrix elements may vary significantly over the zone face, so some error is introduced in the comparison which will, however, be small if the two points are close. In spite of these difficulties, it is desirable to estimate the OPW form factors from previous band calculations as a check on our calculations. In the case of calcium, for which there do not exist any previous band calculations, we will compute the Fermi surface in some detail from our OPW form factors.

### 1. Lithium

The Hartree-Fock wave functions for lithium were taken from Holöien<sup>8</sup>; the Hartree-Fock parameters were taken from Fock and Petrashen.<sup>9</sup> For both lithium and beryllium, analytic approximations to the wave functions were given which greatly simplified the numerical work. In addition, the presence of only the 1s state in the core reduced the computations required.

Only very rough comparison is possible with previous band calculations in the monovalent metals. The Fermi surface does not intersect any zone face, so the splittings corresponding to OPW form factors have not been obtained. However, the Fermi surface approaches rather close to a (110) zone face near the point *N*. Therefore, rough comparison may be made between computed splittings at *N* and the OPW form factor corresponding to  $q=2k_F$ . We compare with "Fourier transforms of the effective potential" computed by Ham<sup>10</sup> from the calculated band splittings at *N*, *P*, and *H*. The comparison appears in Table II. The differences between values given by Ham from different symmetry points

shows that there are sizable variations of the matrix elements over the zone face, as he has indicated, and that comparisons of our values with the symmetry-point splittings are not very reliable. It also emphasizes the importance, for computing properties, of obtaining matrix elements between states on the Fermi surface as we have done rather than at symmetry points. In the alkalis, the comparison at *N* is more significant than the others, but still corresponds to a transform with wave number differing by 10% from that in our calculation. We regard the agreement as suitable in view of this difference.

### 2. Beryllium

Hartree-Fock wave functions were taken from Holöien,<sup>8</sup> but since published Hartree-Fock parameters were not found for Be<sup>++</sup>, the computation was carried through without exchange. All other metals have been treated including exchange. Hartree parameters were taken from Hartree and Hartree.<sup>11</sup>

Comparison is made with the band calculation of Herring and Hill.<sup>12</sup> Form factors were obtained from our calculation for beryllium and for the other polyvalent metals by linear extrapolation between  $q=1.5k_F$  and  $q=2k_F$ . The comparison appears in Table II. Values for the (100) form factor were obtainable from both *K* and *M*; *K* lies nearer the Fermi surface and is therefore listed first. Only two band energies were given at *H*, so it was necessary to take the (100) form factor from *K* in order to deduce the (110) value. The rather large discrepancies are presumably due to the influence of higher bands; a few-OPW treatment of the band structure is rather inadequate when the form factors are as large as they are in beryllium.

### 3. Sodium

Hartree-Fock wave functions and parameters were obtained from Hartree and Hartree.<sup>13</sup> In sodium, and

<sup>11</sup> D. R. Hartree and W. Hartree, Proc. Roy. Soc. (London) **A149**, 210 (1935).

<sup>12</sup> C. Herring and A. G. Hill, Phys. Rev. **58**, 132 (1940).

<sup>13</sup> D. R. Hartree and W. Hartree, Proc. Roy. Soc. (London) **A193**, 299 (1948).

<sup>8</sup> E. Holöien, Proc. Phys. Soc. (London) **A68**, 297 (1955).

<sup>9</sup> V. Fock and M. J. Petrashen, Phys. Z. Sowjet. **8**, 547 (1935).

<sup>10</sup> F. S. Ham, Phys. Rev. **128**, 2524 (1962).

in the remaining metals, all integrations were performed numerically by hand. In the integrations the region was divided into twenty to thirty intervals. Approximately one day of computation was required for sodium. As in the case of lithium, comparison is made with the splittings found by Ham.<sup>10</sup>

#### 4. Magnesium

Hartree-Fock wave functions and parameters were obtained from Yost.<sup>14</sup> We compare our OPW form factors with values obtained from the band energies at symmetry points computed by Falicov.<sup>15</sup> Values for the (100) form factor are listed in order of proximity to the Fermi surface of the symmetry point in question. Agreement is remarkable; it should be noted, however, that the band energies at  $H$  do not differ from the Fermi energy much more than those at  $K$ , so a comparison with the (100) value determined at  $H$  is about as appropriate as with the value from  $K$ . We might also compare the discrepancies with the errors inherent in band calculations, which Falicov<sup>15</sup> has attempted to reduce to 0.03 Ry.

#### 5. Aluminum

Calculations were based on the Hartree-Fock treatment of the  $\text{Al}^{3+}$  ion by Froese.<sup>16</sup> We compare with the splittings computed both by Heine<sup>17</sup> and Segall.<sup>18</sup> Heine's values at  $K$  have not been included because of an apparent numerical error in the third-band energy.<sup>18,19</sup> The agreement with the values at  $W$ , which lies quite close to the Fermi surface, is quite good, and comparable to the discrepancies between the two band calculations. We note that, even in aluminum, estimates based upon the different symmetry points differ by about 0.01 Ry.

#### 6. Potassium

The Hartree-Fock calculations for  $\text{K}^+$  by Hartree and Hartree<sup>20</sup> were used, and again comparison is made with estimates from the band calculation by Ham.<sup>10</sup>

#### 7. Calcium

Calculations were based upon the Hartree-Fock treatment of  $\text{Ca}^{++}$  by Hartree and Hartree.<sup>21</sup> There has apparently not been a previous band calculation for calcium, and our examination of band energies at symmetry points for the other metals suggests that a tabulation of the energies at symmetry points estimated

from the form factors would not be particularly reliable. It is of some interest, however, to determine the Fermi surface of calcium. This we can do from the form-factor curve for calcium. The calculation is given in Appendix B, along with preliminary comparison with experiment.

#### 8. Copper

Copper was treated only for comparison with the other metals. The assumption that the core states are the same as in the atom is completely inadequate for copper, where the conduction and  $d$  bands are intimately mixed. Further, the entire perturbation treatment is questionable when the bands are as seriously deformed as in copper. However, we may proceed just as in the other metals to obtain a form factor. We have used the Hartree-Fock treatment of the  $\text{Cu}^+$  ion given by Piper.<sup>4</sup>

As in the alkali metals we compare the form factor for  $q=2k_F$  to the splitting at the center of the nearest zone face, in this case at the point  $L$ . We find a negative value, implying that the even state lies lower, whereas the band calculation of Segall<sup>22</sup> gives the odd state lower. This confirms our misgivings at the start and, in fact, the comparison of copper with the other metals does not seem very informative.

#### 9. Zinc

The form-factor curve was taken directly from our earlier treatment,<sup>2</sup> which was almost identical to that described here. There was no previous band calculation to compare with, but a comparison<sup>8</sup> with the observed Fermi surface suggested agreement comparable to the agreement we find with the other metals.

### IV. A SIMPLE MODEL AND TRENDS IN THE PERIODIC TABLE

We find that it is possible to account remarkably well for the OPW form factors we have computed in terms of a simple model with a single adjustable parameter. We note that the main attractive contribution to the effective potential comes from the long-range Coulomb field of the net ion charge,  $Ze$ . The remaining contributions (except for screening) are restricted to the core and may be approximated by a delta function. Of these localized terms, the largest arises from the orthogonalization terms so the delta function is positive. We screen these with a Hartree dielectric function for free electrons of the density in question. Thus, we approximate the OPW form factor by

$$v(q) = (-4\pi Ze^2/q^2 + \beta)/\Omega_0\epsilon(q). \quad (4)$$

$\beta$  is the strength of the delta-function repulsion.

Clearly, because of the operator nature of the repulsive term,  $\beta$  may depend upon the Fermi wave number and, therefore, upon the atomic volume. We

<sup>14</sup> W. J. Yost, Phys. Rev. **58**, 557 (1940).

<sup>15</sup> L. M. Falicov, Phil. Trans. Roy. Soc. **A255**, 55 (1962).

<sup>16</sup> C. Froese, Proc. Cambridge Phil. Soc. **53**, 210 (1957).

<sup>17</sup> V. Heine, Proc. Roy. Soc. (London) **A240**, 361 (1957).

<sup>18</sup> B. Segall, Phys. Rev. **124**, 1797 (1961).

<sup>19</sup> W. A. Harrison, Phys. Rev. **118**, 1182 (1960).

<sup>20</sup> D. R. Hartree and W. Hartree, Proc. Roy. Soc. (London) **A166**, 450 (1938).

<sup>21</sup> D. R. Hartree and W. Hartree, Proc. Roy. Soc. (London) **A164**, 167 (1938).

<sup>22</sup> B. Segall, Phys. Rev. **125**, 109 (1962).

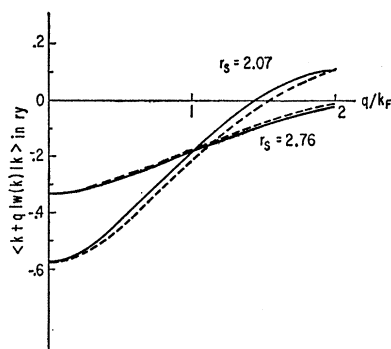


FIG. 3. The OPW form factor for aluminum calculated at the observed density ( $r_s=2.07$ ) and in an expanded crystal

( $r_s=2.76$ ).

Dashed lines are the corresponding curves computed from the model potential with  $\beta=36.6$  Ry-a.u.<sup>3</sup>.

will first test the validity of the wave-number dependence implied by Eq. (4) for the observed atomic volume. We will then examine the dependence of  $\beta$  on the atomic volume.

In Fig. 3 we have shown again the computed form-factor curve for aluminum ( $r_s=2.07$ ). We also show Eq. (4) plotted with  $\beta$  adjusted to fit at  $q$  equal to  $2k_F$ . The fit is extremely good (within about 0.03 Ry) over the entire wave number range. Similar fits to the other metals have been made. The corresponding values of  $\beta$  are listed in Table III. In all cases, except copper, the agreement with our computed curves is comparable.

It should be pointed out that for treating a band structure per se, the increased accuracy of the full calculation is rather important. However, for treating electronic properties the approximate form should be quite adequate. It should also be pointed out that, as we found in zinc,<sup>2</sup> the breakdown of the simple-potential approximation gives variations in matrix elements of about a tenth of a rydberg when we consider interaction of states which do not both lie on the Fermi surface. This shortcoming was also apparent in variations in form factors estimated from the splitting at various symmetry points in Table II. Thus, it is not reasonable to extend the use of this potential to the atomic properties.

The most striking aspect of the values for  $\beta$  listed in Table III is the lack of any trend with atomic number or with valence. Even in the alkali metals there is no trend, and the familiar lowering of the  $s$  state at the zone face with atomic number, which corresponds to the very apparent dropping of the form factor curves in Fig. 2, is due to the increase in atomic volume with atomic number rather than to changes in the effective core potential. This lack of trend in the  $\beta$  values manifests itself in the striking similarity of all of the form-factor curves of Fig. 2 for the polyvalent metals,

TABLE III. The strength,  $\beta$ , of the repulsive pseudopotential in units of rydbergs—atomic units of volume.

Li, 29.1	Be, 30.8	
Na, 27.0	Mg, 41.6	Al, 36.6
K, 31.5	Ca, 50.6	
Cu, 2.2	Zn, 26.5	

where there does not exist this marked dependence of atomic volume on atomic number.

We now consider the variation of  $\beta$  with atomic volume for a given metal. In Fig. 3 we show the OPW form factor for aluminum with an expanded volume corresponding to an increase in  $r_s$  by a factor of  $\frac{4}{3}$ . (The form factor in this case was computed for  $q/k_F=0, \frac{2}{3}, \frac{4}{3}, \text{ and } 2$ .) We also show Eq. (4) plotted for the increased volume with the value of  $\beta$  chosen for the normal volume. Clearly, the same value of  $\beta$  accounts rather well for both densities, though a 14% decrease in  $\beta$  would be required to make the fit exact at  $2k_F$ . Thus, Eq. (4) may be used, at least for aluminum, with a single value of  $\beta$  over rather large variations in atomic volume and very little error is introduced.

We have not made the corresponding comparison for the other metals, but we can find an indication by considering Ham's<sup>10</sup> band calculations on the alkali metals. As we indicated above, we may obtain an estimate of the OPW form factor for  $q=2k_F$  from the splitting at  $N$  (between the states  $N_1$  and  $N_1'$ ). Ham<sup>10</sup> has listed these splittings as a function of atomic volume for the alkalis and we may, therefore, make an estimate of  $\beta$  as a function of atomic volume. This estimated  $\beta$  drops as the atomic volume drops in all cases (in contrast to aluminum), but the size of the variations for lithium and sodium are comparable to those in aluminum. For potassium, and particularly for rubidium and cesium, the drop in  $\beta$  is very rapid at small volumes. It seems likely that this drop is associated with the depression of the even state by the incipient  $d$  band, rather than with a real drop in the matrix elements derivable from the OPW form factor. With increasing atomic number the  $d$  band, and the  $N_2$  state in particular, drops. Furthermore, for a given element, the  $d$  band drops as the atomic volume is decreased. Strictly speaking, an  $N_2$  state cannot interact with an  $N_1$  state, but their proximity indicates a strong interaction between the plane waves from which they are derived. Thus, we would say that the band gaps at  $N$  are not given well by the OPW form factor for the alkali metals of high atomic number, but the form factors themselves may still be describable by Eq. (4) with values of  $\beta$  comparable to those of the light metals and these may not be inordinately sensitive to changes in volume.

The results for the alkalis are consistent with our suggestion of a  $\beta$  which does not vary significantly with atomic number or atomic volume, but do not lend strong support to the suggestion. Further, these results give a warning against too literal an application of form factors to the band structures in the heavy elements. Equation (4) would indicate that the form factors at  $q=2k_F$  become less negative in the heavy alkali metals as the volume is decreased whereas the band gaps apparently become more negative.<sup>23</sup>

<sup>23</sup> The author is indebted to Dr. F. S. Ham for pointing out to him this discrepancy in the alkali metals.

### V. CONCLUSIONS

We have presented a rather simple scheme for computing the OPW form factors for metals from the Hartree-Fock calculations on the corresponding ion and applied this to a series of metals of low atomic number. The results are sufficiently similar to that obtained earlier<sup>2</sup> for zinc, that we expect the treatment of electronic properties in terms of these curves to be quite adequate for all of these metals, as we found it to be in zinc. The direct application of the technique to copper was quite unsuccessful, and indicates that the approach is not applicable to the noble metals.

The comparison with existing band calculations given in Table II was rather informative. There are two approximations implicit in relating the OPW form factor to the band splittings at symmetry points. First is the assumption that the matrix element between any two plane waves differing in wave number by  $q$  is the same as that when both initial and final wave numbers lie on the Fermi surface. We found explicitly in zinc<sup>2</sup> that this is not the case, and the errors become more serious as we move further from the Fermi surface. Second, we neglect the effect of neighboring bands: These give shifts of the order of the square of the matrix element divided by the energy difference from the band in question, and are not always negligible. The discrepancies we found between our values and estimates from the symmetry points were no bigger than the differences between values of the same form factor obtained from different symmetry points. Furthermore, the discrepancies were smallest for the symmetry points lying closest to the Fermi surface, and were of the order of a hundredth of a rydberg there. Thus, the band calculations generally may be regarded as confirming our calculations.

The fact that the discrepancies become small for the symmetry points closest to the Fermi surface suggests that the main errors in computing symmetry-point energies from the OPW form factors comes from the wave-number-independent pseudopotential approximation rather than the inclusion of only a few plane waves. We may note from Table II that the associated errors are larger in the alkali metals than in the polyvalent metals, but not significantly larger. A cursory look at the heavier alkalis suggests that neglect of interaction with higher bands becomes increasingly serious at higher atomic numbers.

The most striking result of our analysis is the degree of success of the simple model for the effective potential with a single parameter for each metal: Particularly, the fact that the model seems to carry over reasonably well to changes in volume. This means that we may directly treat alloys in a simple manner, including the distortions of the lattice due to alloying if they are known: Computations of resistivity or of band structure become very direct.

Another striking finding is the apparent lack of

trends in the repulsive term in the potential which arises from the ion core. It was natural to expect a uniform lowering of  $s$ -like states in comparison to  $p$ -like states with increase of atomic number, since this was known to occur in the alkali metal series. We find that that tendency does not occur in the polyvalent metals, and that in the alkalis it is largely due to the increase in atomic volume with atomic number: In the heavier alkali metals there appears to be an additional depression of the  $s$  state from higher bands which drop as the atomic number increases.

It is interesting to indicate the degree of reliability of the delta-function strengths,  $\beta$ , given in Table III. We regard our OPW form-factor curves as reliable to one or two hundredths of a rydberg; similarly, the values obtained from the effective potential are reliable to this order. Since the atomic volumes are of the order of a hundred a.u.,<sup>3</sup> and the dielectric function of the order of one when  $q$  is near  $2k_F$ , we see from Eq. (4) that the  $\beta$  values are reliable to the order of 5. In view of the sizable variations from element to element, this is sufficiently accurate to allow very informative studies of the properties of the corresponding alloys.

### ACKNOWLEDGMENT

The author is indebted to Mrs. E. L. Fontanella for assistance in the computations for magnesium, potassium, and copper.

### APPENDIX A: PROCEDURE FOR CALCULATION OF THE OPW FORM FACTORS

The right-hand side of each numbered equation below is a mathematical operation which is carried out. Values obtained for aluminum are given in square brackets at each step. All energies are in rydbergs, other parameters are in atomic units. All integrals over  $r$  run from zero to infinity.

For the observed volume,  $\Omega_0$ , we compute

$$4\pi/\Omega_0[0.1128],$$

radius of the equivalent sphere,  $r_0[2.985]$ , and free-electron Fermi wave number,  $k_F[0.9273]$ . From a Hartree-Fock treatment of the ion we obtain the normalized radial wave functions,  $P_{nl}(r)$ , and parameters,  $\epsilon_{nl,ni}$ .

$$\langle k|\psi_{nl}\rangle = \left(\frac{4\pi}{\Omega_0}\right)^{1/2} \int r j_l(kr) P_{nl}(r) dr; \quad (A1)$$

$$[1s, 0.032; 2s, -0.234; 2p, 0.0816].$$

$$\begin{aligned} \sum_t \langle \mathbf{k} + \mathbf{q} | t \rangle \langle t | \mathbf{k} \rangle \\ = \sum_l (2l+1) P_l(\cos 2\Theta) \sum_n \langle k | \psi_{nl} \rangle^2; \quad (A2) \\ [0.0560 + 0.0200 \cos 2\Theta]. \end{aligned}$$

$$\begin{aligned} v_q^{(0)} = \sum_t \langle \mathbf{k} + \mathbf{q} | t \rangle \langle t | v_{op}' | \mathbf{k} \rangle \\ = \sum_l (2l+1) P_l(\cos 2\Theta) \sum_n \langle k | \psi_{nl} \rangle^2 \\ \times (-|\epsilon_{nl,ni}| - k_F^2); \quad (A3) \\ [-0.844 - 0.196 \cos 2\Theta]. \end{aligned}$$

We select a set of  $q$  values for which we will compute the form factor. All computations will be made for these  $q$ 's and for  $q=0$  if the corresponding value is not infinite.

$$\begin{aligned} [q/k_F=0, 0.5, 1, 1.5, 2], \\ \cos 2\Theta = 1 - q^2/2k_F^2, \\ [1, 0.875, 0.5, -0.125, -1]. \end{aligned} \quad (\text{A4})$$

Expressions (A2) and (A3) above are evaluated for the  $q$ 's in question:

$$\begin{aligned} [0.0760, 0.0735, 0.0660, 0.0535, 0.0360; \\ -1.040, -1.016, -0.942, -0.820, -0.648]. \end{aligned}$$

We define  $U(r) = 4\pi r^2 \rho_0(r)$ , where  $\rho_0$  is the core-electron density. If  $U(r)$  is not tabulated, we compute

$$U(r) = \sum_{l,n} 2(2l+1) P_n^l(r). \quad (\text{A5})$$

The Fourier transform of the electron density is proportional to

$$n(q) = \int \left( \frac{\sin qr}{qr} \right) U(r) dr; \quad (\text{A6})$$

$$[10, 9.90, 9.52, 8.95, 8.24].$$

Note  $n(0) = \sum_{n,l} 2(2l+1)$  is equal to the number of core electrons.

The Fourier transform of the ion potential is proportional to

$$\begin{aligned} v_q^{(1)} = (4\pi/\Omega_0) (2/q^2) [-Z - n(0) + n(q)], \\ [-, -3.253, -0.913, -0.472, -0.312], \end{aligned} \quad (\text{A7})$$

where  $Z$  is the valence [3]. For  $q=0$  the integral is restricted to the equivalent sphere;

$$v_0^{(1)} = \left( \frac{-4\pi}{\Omega_0} \right) \left( Zr_0^2 + \frac{1}{3} \int r^2 U dr \right). \quad (\text{A8})$$

The Fourier transform of the exchange potential is proportional to

$$v_q^{(2)} = -\frac{1.2707}{q} \frac{4\pi}{\Omega_0} \int \sin qr [rU(r)]^{\frac{1}{2}} dr; \quad (\text{A9})$$

$$[-0.377, -0.343, -0.262, -0.172, -0.105].$$

The Fourier transform of the potential arising from orthogonalization is proportional to

$$v_q^{(3)} = -\frac{4\pi}{\Omega_0} \frac{2Z n(q)}{q^2 n(0)} \sum_t \langle \mathbf{k} | t \rangle \langle t | \mathbf{k} \rangle; \quad (\text{A10})$$

$$[-, -0.237, -0.057, -0.024, -0.012].$$

$$\langle k | u | k \rangle = v_0^{(1)} + v_0^{(2)} - v_0^{(0)}; \quad (\text{A11})$$

$$[-2.473].$$

$$v_q^{(4)} = \frac{\langle \mathbf{k} | u | \mathbf{k} \rangle}{1 - \sum_t \langle \mathbf{k} | t \rangle \langle t | \mathbf{k} \rangle} \sum_t \langle \mathbf{k} + \mathbf{q} | t \rangle \langle t | \mathbf{k} \rangle; \quad (\text{A12})$$

$$[-0.203, -0.197, -0.177, -0.143, -0.096].$$

That contribution to the screening field which arises directly from the non-Hermiticity of the pseudo-potential is given by

$$v_q^{(5)} = \frac{4\pi}{\Omega_0} \frac{2Z}{q^2} \sum_t \langle \mathbf{k} + \mathbf{q} | t \rangle \langle t | \mathbf{k} \rangle; \quad (\text{A13})$$

$$[-, 0.231, 0.052, 0.019, 0.007],$$

divided by the Hartree dielectric function for free electrons,  $\epsilon(q)$ .

$$\epsilon(q) = 1 + \frac{1}{2\pi k_F} \frac{1}{\eta^2} \left\{ \frac{1-\eta^2}{2\eta} \ln \left| \frac{1+\eta}{1-\eta} \right| + 1 \right\}; \quad (\text{A14})$$

$$[-, 6.375, 2.252, 1.478, 1.172];$$

where  $\eta = q/2k_F$ . The dielectric function for other metals may be computed from that for aluminum according to

$$\epsilon(q/k_F) = 1 + [\epsilon(q/k_F)_{\text{Al}} - 1] (0.9273/k_F).$$

The OPW form factor is

$$\begin{aligned} \langle \mathbf{k} + \mathbf{q} | w(k) | \mathbf{k} \rangle \\ = [v_q^{(1)} + v_q^{(2)} + v_q^{(3)} + v_q^{(4)} + v_q^{(5)} - v_q^{(0)}] / \epsilon(q); \end{aligned} \quad (\text{A15})$$

$$[-0.573, -0.427, -0.183, +0.019, +0.113].$$

The  $q=0$  value is simply  $-2k_F^2/3$ .

In the absence of a Hartree-Fock calculation for the ion, Hartree parameters may be used in Eq. (A3) and  $v_q^{(2)}$  is taken equal to zero.

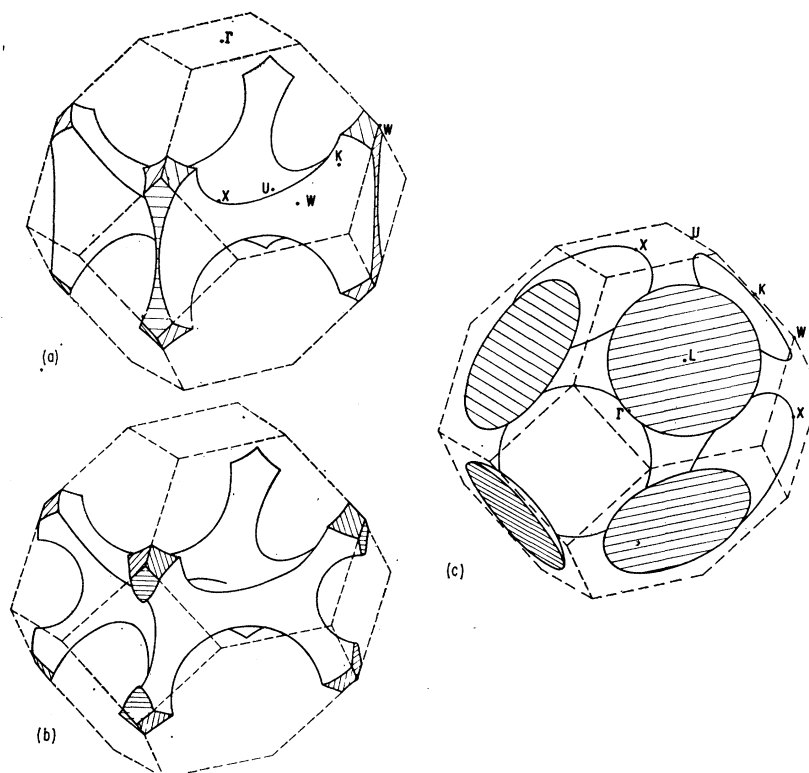
## APPENDIX B: THE FERMI SURFACE IN CALCIUM

Calcium is face-centered cubic with unit cube edge of  $a = 10.5$  a.u. Zone faces intersect the Fermi surface corresponding to lattice wave numbers of type  $[111]2\pi/a$ , and  $[200]2\pi/a$ . The OPW form factors to be associated with these faces are 0.003 and 0.039 Ry, respectively. If the (111) gap is, in fact, as small as this, magnetic breakdown<sup>24</sup> will occur at high fields. (At the breakdown field<sup>3</sup> of  $H = \pi m c V_q^2 k_F / e \hbar E_{Fq}$ , which is 50 kG for  $V_q$  equal to 0.003 Ry and the other parameters taken for calcium, the probability of jumping the gap is  $1/e$ .) Our calculation is not sufficiently precise to be sure even of the order of magnitude of this breakdown field, but we should consider a high-field and a low-field Fermi surface.

At low fields, both types of zone face are effective. Except for the change in connectivity of the surface, the distortion of the surface by the (111) face is negligible: The effect of the (200) faces are readily included by treating a two-by-two Hamiltonian matrix. In Fig. 4 is shown the resulting Fermi surface, as well as the free-electron surface for a divalent *fcc* metal. Because of the smallness of the gap on the (111) faces, the second-band electron surface is essentially the same

<sup>24</sup> M. H. Cohen and L. Falicov, Phys. Rev. Letters **5**, 544 (1960); **7**, 231 (1961).

FIG. 4. The calculated low-field Fermi surface in calcium; (a) and (c) are the first- and second- band surfaces in the one OPW, or nearly-free-electron approximation; (b) is the first-band surface from our calculation; the second-band surface is essentially unchanged by our calculation.



as that for free electrons. The main effect of the finite lattice potential on first-band hole surface is to open gaps in the thin sections of the free-electron surface. The resulting hole surface has the connectivity of the third-band electron surface in aluminum. The introduction of interaction with a second plane wave also shifts the Fermi energy by about a percent. If we correct for this shift, to obtain a surface of the correct volume, this reduces the sensitive cross section (f) described below by about 14%, and affects the others by smaller amounts. We have neglected this correction.

We may list the sections of the surface which are most interesting from an experimental point of view. The corresponding estimated areas and de Haas-van Alphen periods are given in Table IV.

(a) The minimum section of a first-band arm, corresponding to orbits in a field in a  $[110]$  direction.

(b) An orbit around the intersection of four arms at  $W$ , as viewed along a  $[100]$  direction.

(c) An orbit around the intersection of four arms at  $W$ , as viewed along a  $[110]$  direction.

(d) An orbit around the second-band disks. The minimum area is seen with fields along a  $[110]$  direction.

(e) Another interesting section of the second-band disks arises with fields parallel to a  $[100]$  direction and has been computed by Berlincourt.<sup>25</sup>

(f) The nearly circular region surrounded by four arms, seen with fields in the  $[100]$  direction.

(g) An approximately square orbit around the outside of these arms and concentric with (f) as viewed along a  $[100]$  direction.

In the high-field limit all of these disappear except (f) and (g), each of which has the same area as above, and no new extremal orbits appear for fields in the  $[100]$  direction. The Fermi surface then becomes the same as that for a monovalent, simple-cubic metal.

Berlincourt<sup>25</sup> observed de Haas-van Alphen oscillations in calcium with a magnetic field parallel to  $[100]$  using fields pulsed to 200 kG. He found a period of  $0.59 \times 10^{-7} \text{ G}^{-1}$ , with an estimated error of 10%, and

TABLE IV. Predicted sections of Fermi surface and De Haas-van Alphen periods for calcium.

Section	Field direction	Area (a.u.)	Period ( $10^{-7} \text{ G}^{-1}$ )
(a)	$[110]$	0.0062	4.3
(b) <sup>a</sup>	$[100]$	0.035	0.76
(c)	$[110]$	0.038	0.71
(d) <sup>a</sup>	$[110]$	0.054	0.50
(e) <sup>a</sup>	$[100]$	0.064	0.42
(f)	$[100]$	0.09	0.30
(g)	$[100]$	0.31	0.085

<sup>25</sup> T. G. Berlincourt, in *Proceedings of the Seventh International Conference on Low-Temperature Physics* (University of Toronto Press, Toronto, 1960).

<sup>a</sup> These orbits occur in the single-OPW approximation, and are not appreciably modified by the lattice potential. Single-OPW areas are listed here.

indication of a period shorter by a factor of about 8. The first does not match any of the periods given in Table IV for  $[100]$  fields very closely, but is of the order of (b), (e), and (f). Neither (b) nor (e) is very sensitive to the size of the form factors and we do not expect errors this large. We would be inclined to guess that the sensitive orbit (f) has been observed. The shorter period agrees nicely with (g) and with no other orbit. These are just the two orbits which remain for high fields in the  $[100]$  direction and suggests that at

the 200 kG which he used, breakdown has become important.

Condon and Marcus<sup>26</sup> and Condon<sup>27</sup> have studied the de Haas-van Alphen effect in fields up to 30 kG and find results consistent with the low-field surface, though quantitative comparison is not complete.

<sup>26</sup> J. H. Condon and J. A. Marcus, *Bull. Am. Phys. Soc.* **6**, 145 (1961).

<sup>27</sup> J. H. Condon (to be published).

## Evidence for the $\langle 110 \rangle$ Swelling Constant Energy Surface for Heavy Holes in Silicon

H. MIYAZAWA, K. SUZUKI, AND H. MAEDA

*Toshiba Central Research Laboratory, Kawasaki, Japan*

(Received 23 April 1963)

A newly devised experimental technique has revealed that the puzzling weak-field anisotropy of the galvanomagnetic effects in  $p$ -type silicon above 77°K belongs, according to our classification, to the last of the four possible types for cubic semiconductors. The strange behavior is ascribable to the growth of the  $\langle 110 \rangle$  swelling energy contour for the heavy-hole band. A brief description is given of the calculation of the nonparabolicity with the recent band parameters and of the calculation of the conductivity tensor for a fictitious energy surface.

**S**YMMETRY arguments predict that only four types can exist for the anisotropy of the weak-field galvanomagnetic effects in cubic semiconductors.<sup>1</sup> These are listed in Table I, together with the corresponding materials and their band shapes, in accordance with the results thus far established.<sup>2</sup> The similarity of the

valence band of silicon and germanium might suggest that  $p$ -type silicon would belong to the third type, as is the case for  $p$ -type germanium. Careful measurements of the weak-field magnetoresistance,<sup>3</sup> however, have disclosed that the anisotropy of the former above liquid-nitrogen temperature is not of the third type and that

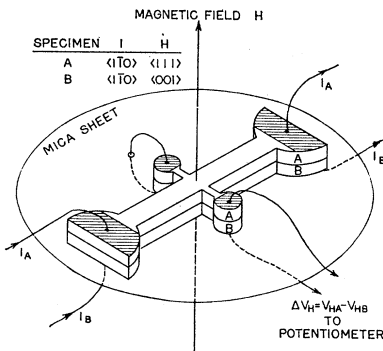


FIG. 1. Principle of the differential method to detect the anisotropy with a low-precision magnet. The merit is in the simultaneous observation of two competing responses within a small space.

<sup>1</sup> H. Miyazawa, in *Proceedings of the International Conference on the Physics of Semiconductors, Exeter* (The Institute of Physics and the Physical Society, London, 1962), p. 636.

<sup>2</sup> G. L. Pearson and H. Suhl, *Phys. Rev.* **83**, 768 (1951); B. Abeles and S. Meiboom, *ibid.* **95**, 31 (1954); M. Shibuya, *ibid.* **95**, 1385 (1954); C. Goldberg, E. N. Adams, and R. E. Davis, *ibid.* **105**, 865 (1957); J. G. Mavroides, and B. Lax, *ibid.* **107**, 1530

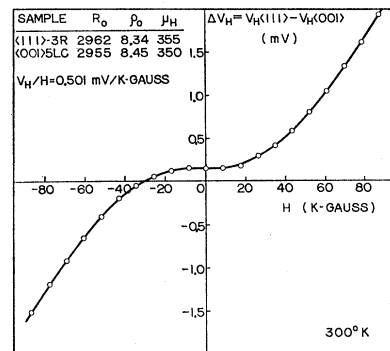


FIG. 2. An experimental result observed by the differential method. The measurement was made with a Bitter-type air core solenoid generating 90-kG maximum field. The result proves that  $R_H(111) > R_H(001)$  at finite fields.

(1957); W. M. Bullis, *ibid.* **109**, 292 (1958); W. E. Krag, *ibid.* **118**, 435 (1960); H. Miyazawa and H. Maeda, in *Proceedings of the International Conference on Semiconductor Physics, 1960* (Czechoslovakian Academy of Sciences, Prague, 1961), p. 169, and *J. Phys. Soc. Japan* **15**, 1924 (1960).

<sup>3</sup> D. Long and J. Myers, *Phys. Rev.* **109**, 1098 (1958).